Tripling the Census of Dwarf AGN Candidates Using DESI Early Data

Ragadeepika Pucha,[1,2] S. Juneau,[3] Arjun Dey,[3] M. Siudek,[4,5] M. Mezcua,[6,4] J. Moustakas,[7] S. BenZvi,[8] K. Hainline,[2] R. Hviding,[9,2] Yao-Yuan Mao,[1] D. M. Alexander,[10,11] R. Alfarsy,[12] C. Circosta,[13,14] Wei-Jian Guo,[15] V. Manwadkar,[16,17] P. Martini,[18,19,20] B. A. Weaver,[3] J. Aguilar,[21] S. Ahlen,[22] D. Bianchi,[23] D. Brooks,[14] R. Canning,[12] T. Claybaugh,[21] K. Dawson,[24] A. de la Macorra,[25] Biprateep Dey,[26,27] P. Doel,[14] A. Font-Ribera,[14,28] J. E. Forero-Romero,[29,30] E. Gaztañaga,[6,12,4] S. Gontcho A Gontcho,[21] G. Gutierrez,[31] K. Honscheid,[18,32,20] R. Kehoe,[33] S. E. Koposov,[34,35] A. Lambert,[21] M. Landriau,[21] L. Le Guillou,[36] A. Meisner,[3] R. Miquel,[37,28] F. Prada,[38] G. Rossi,[39] E. Sanchez,[40] D. Schlegel,[21] M. Schubnell,[41,42] H. Seo,[43] D. Sprayberry,[3] G. Tarlé,[42] and H. Zou[15]

2411.00091v2
ApJ? Accepted

Dark Energy Spectroscopic Instrument (DESI) survey:
5000 fibers d1.5", 4m KPNO, 3600-9800 A, R=2000-5500

Мотивация – поиск маломассивных ЧД в ядрах галактик, для тестов моделей формировани первоначальных ЧД (“seed formation models”)
Споры о мастшабных соотношениях пи малых массах

DESI early relise+20% of Year 1 data+Legacy DR9

410,757 line-emitting galaxies

BPT-> AGN in 75,928 (≈25.6%) high-mass (log(M⁊/M⊙)> 9.5)
2,444 (≈2.1%) dwarf (log(M⁊/M⊙)≤ 9.5)

Baldassare et al. (2020) extended the $M_{\rm BH}-\sigma_\star$ relation down to $\log(M_\star/{\rm M}_\odot)\approx 8.96$. They found that the dwarf galaxies are in good agreement with the extrapolation of the existing relation (Kormendy & Ho 2013). In contrast, using a sample of 127 low-mass Seyfert 1 galaxies, Martín-Navarro & Mezcua (2018) found a flattening at the low-mass end of the $M_{\rm BH}-\sigma_\star$ relation. Measuring $\sigma_\star$ in low-mass systems is difficult to extend to a larger sample and to farther distances due to the faintness of targets and the limitations of current telescopes and instrumentation. Therefore, even though the $M_{\rm BH}-\sigma_\star$ relation usually shows the tightest correlation, the $M_{\rm BH}-M_\star$ relation is preferred for both extending the scaling relations to lower galaxy masses and/or for comparing to higher redshifts.

(масса хуже, но проще, чем дисперсия)

Stellar mass – SED fitting (CIGALE)

SED: g, r, z, W1, W2, W3,W4 + spectroscopic z
stars+dust+AGN+nebular emission

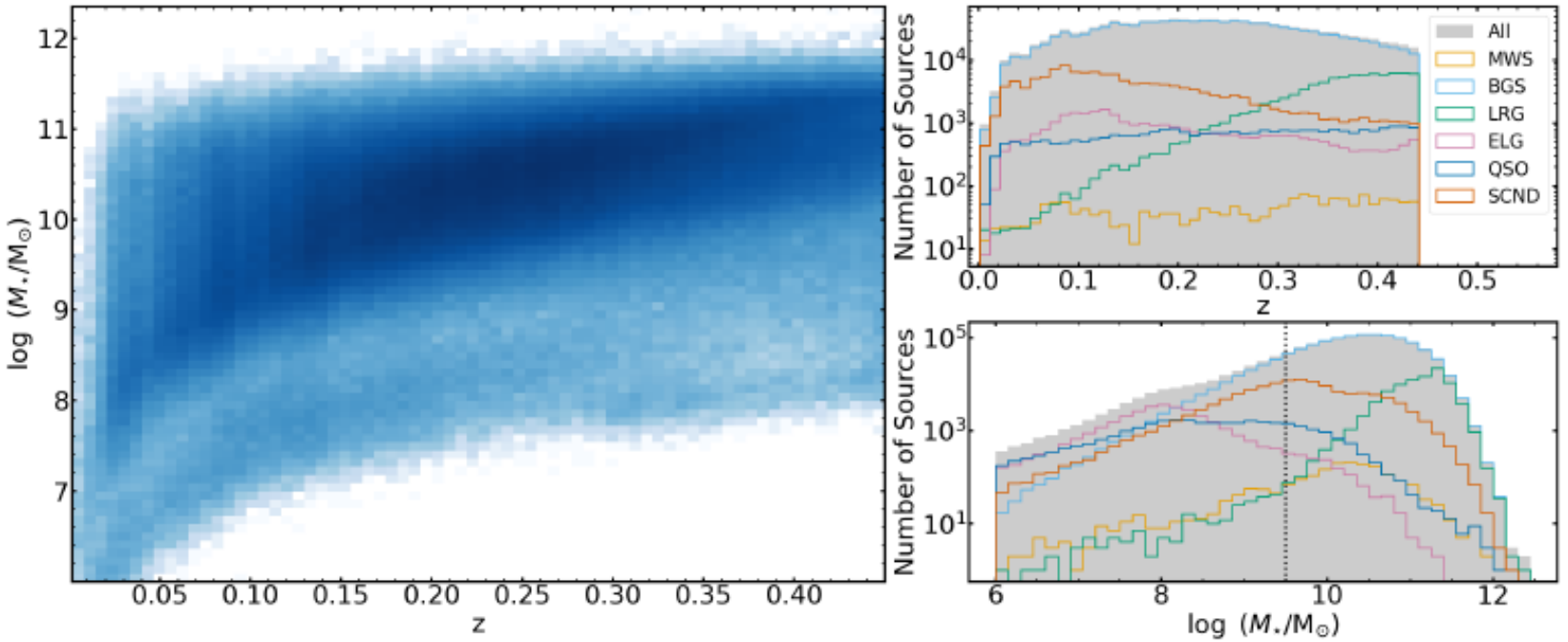

Карлики (меньше, чем БМО): log(M⁊/M№≤ 9.5

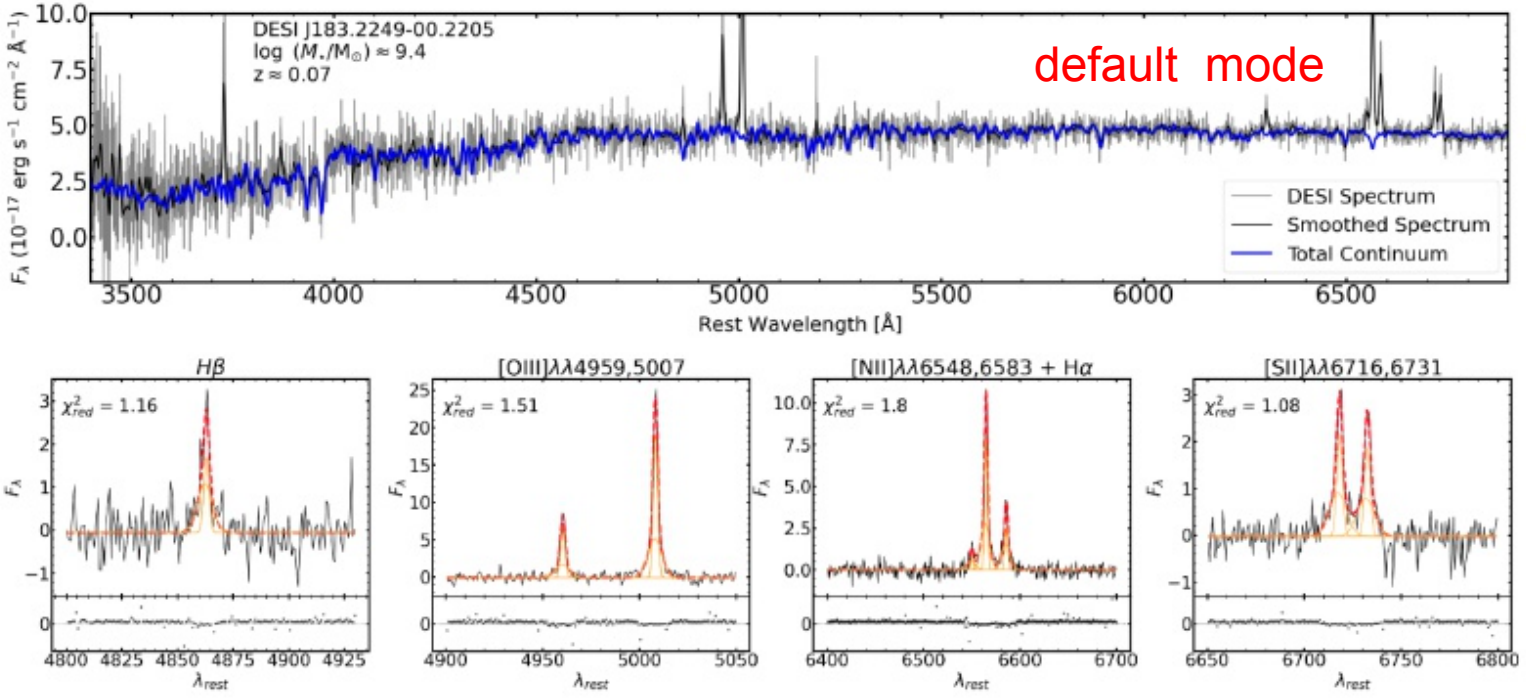

Выбор 1 или 2 компонентов – сперва по [SII]

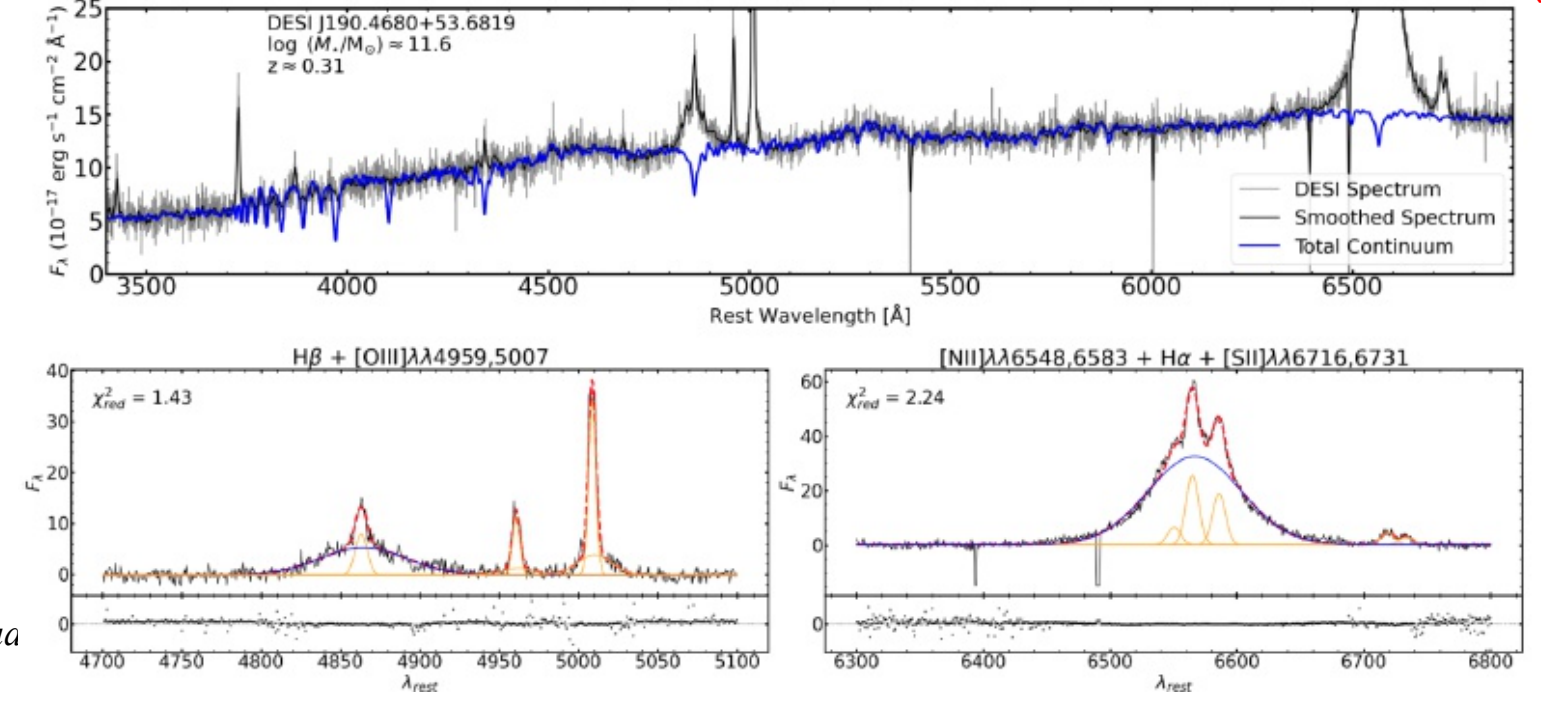

Критерий – эмиссия Na дотягивается до [SII]

Семина

Выделение AGN

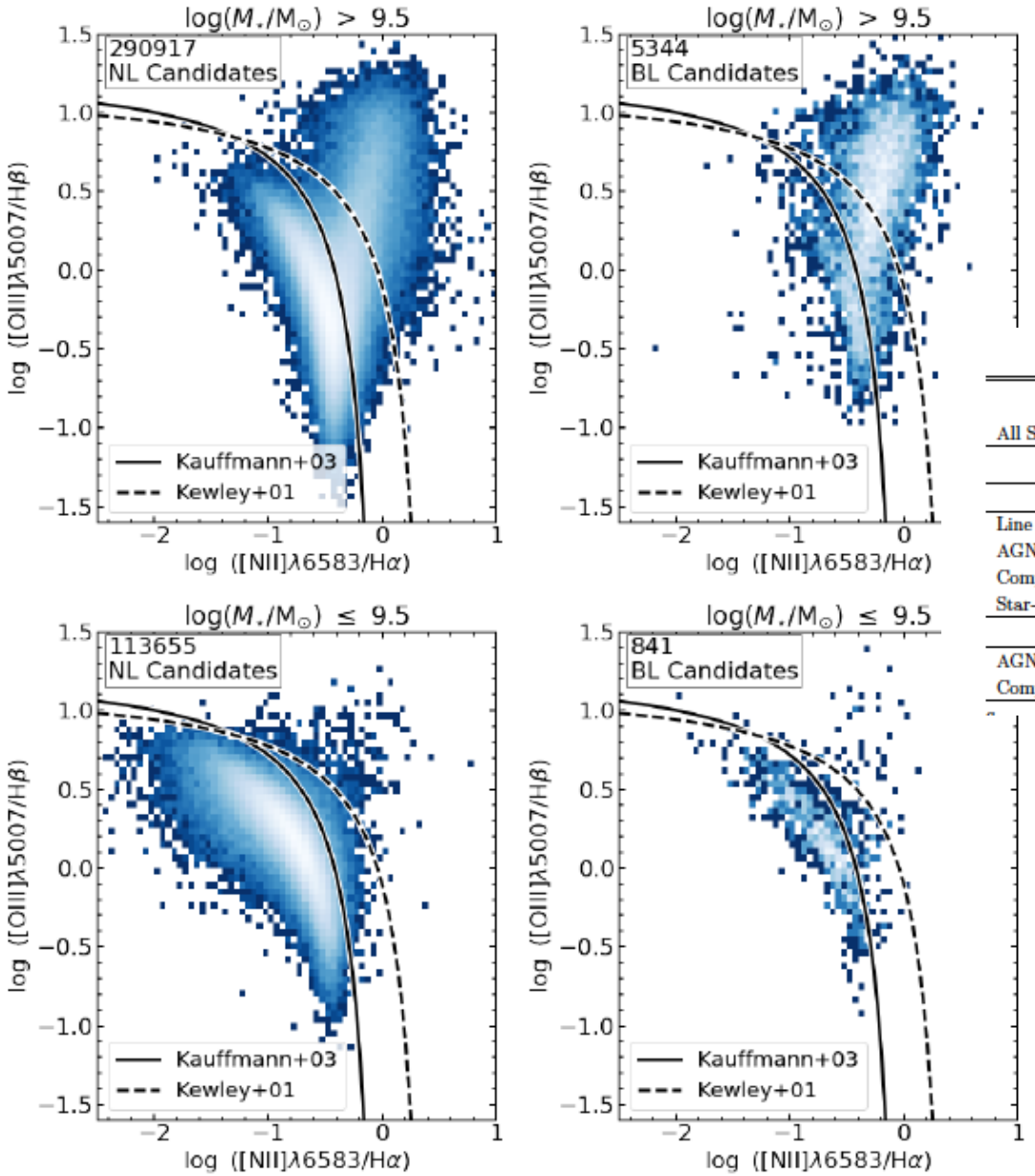

AGN=AGN+composite
(отсюда такой большой процент ~ 26%)

Table 1. Number of AGN, Composites, and Star-Forming Candidates from the BPT Diagram

	Dwarf ($\log(M_\star/M_\odot) \leq 9.5$) Galaxies		**High-Mass ($\log(M_\star/M_\odot) > 9.5$) Galaxies**	
All Sources	221,778		1,128,334	
	NL Candidates	**BL Candidates**	**NL Candidates**	**BL Candidates**
	Before Visual Inspection[a]			
Line Emitting Galaxies	113,655	841	290,917	5,344
AGN Dominated Sources	350 (0.3%)	55 (6.5%)	21,322 (7.3%)	2,905 (54.4%)
Composites	1,933 (1.7%)	106 (12.6%)	50,330 (17.3%)	1,371 (25.6%)
Star-Forming	111,372 (98.0%)	680 (80.9%)	219,265 (75.4%)	1,068 (20.0%)
	After Visual Inspection[b]			
AGN Dominated Sources	365 (0.3%)	40 (4.8%)	21,405 (7.4%)	2,822 (53.6%)
Composites	1,951 (1.7%)	88 (10.7%)	50,470 (17.3%)	1,231 (23.6%)

Сравнение с другими волоконными обзорами

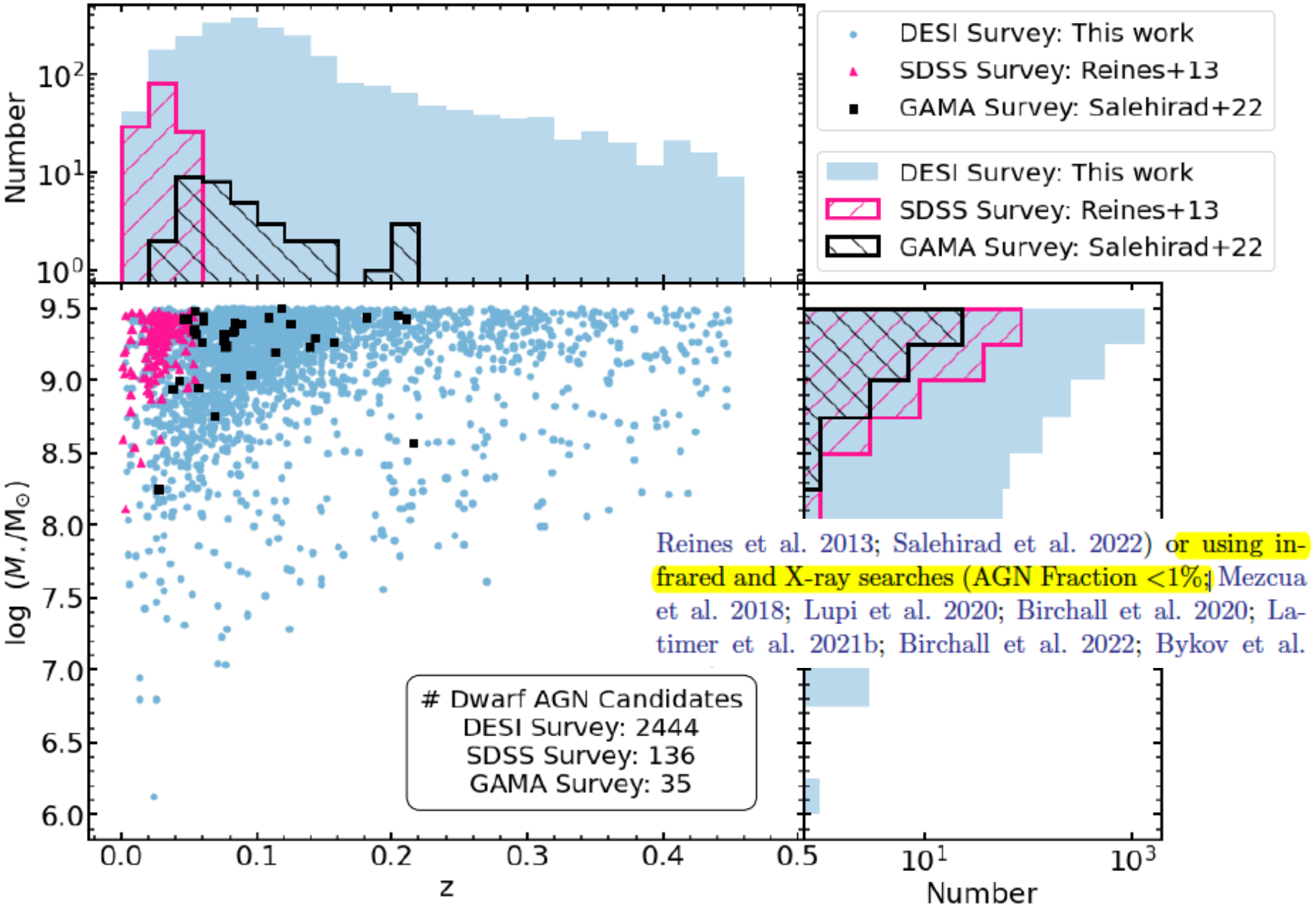

Reines et al. 2013; Salehirad et al. 2022) or using infrared and X-ray searches (AGN Fraction <1%; Mezcua et al. 2018; Lupi et al. 2020; Birchall et al. 2020; Latimer et al. 2021b; Birchall et al. 2022; Bykov et al.

Доля AGN

Растет с массой, хотя эффекты селекции имеют место быть. И это для галактик с эмиссиями

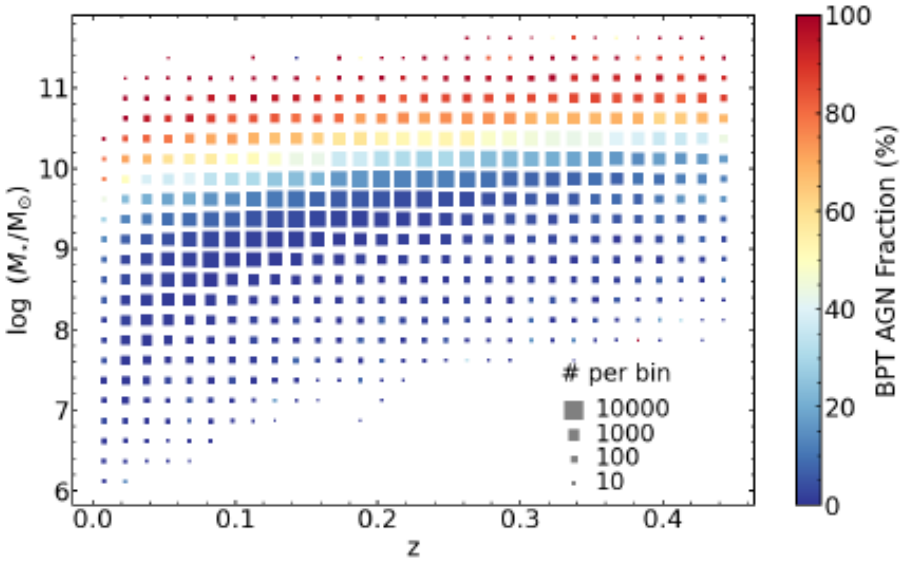

bar. We find that the BPT-AGN fraction, on average, increases with increasing stellar mass, across the entire redshift range, which is consistent with previous optical emission-line studies (e.g., Juneau et al. 2011). The BPT-AGN fraction is $\lesssim$10% at low stellar masses ($\log(M_\star/M_\odot) \leq 9$), and reaches $\approx$100% at high stellar masses ($\log(M_\star/M_\odot) \geq 11$). At $\log(M_\star/M_\odot) \approx 10$, the BPT-AGN fraction appears to decrease with increasing redshift. The change with redshift is unclear at lower and higher masses than this region. We discuss the vari-

Figure 6. 2D-Distribution of line-emitting galaxies in the $\log(M_\star/M_\odot)$ z space color coded by the BPT-AGN fraction within t to the total r

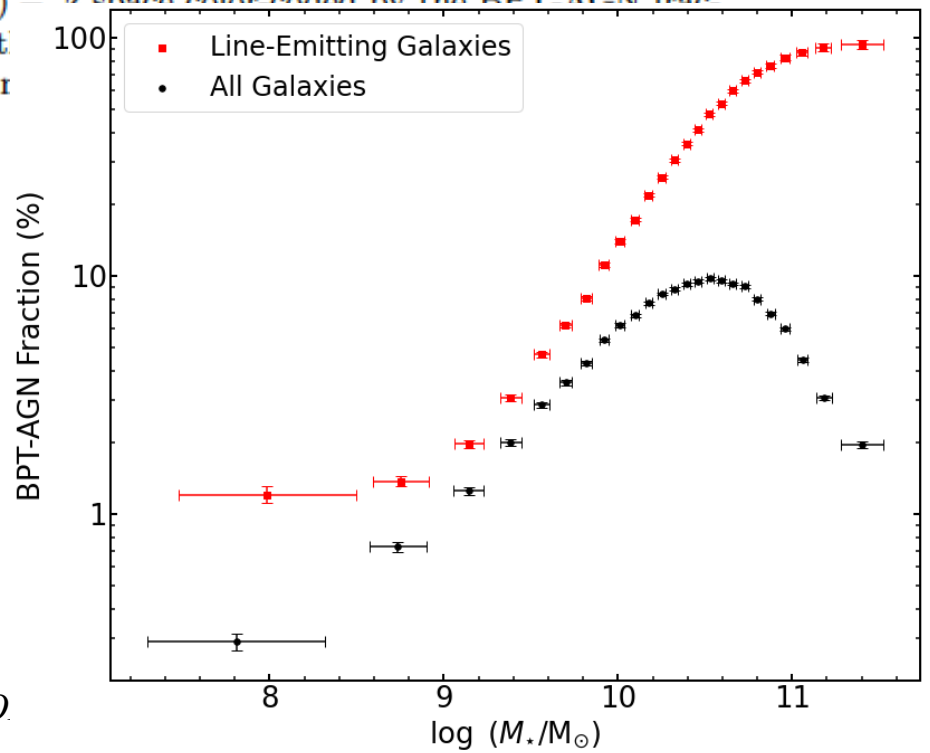

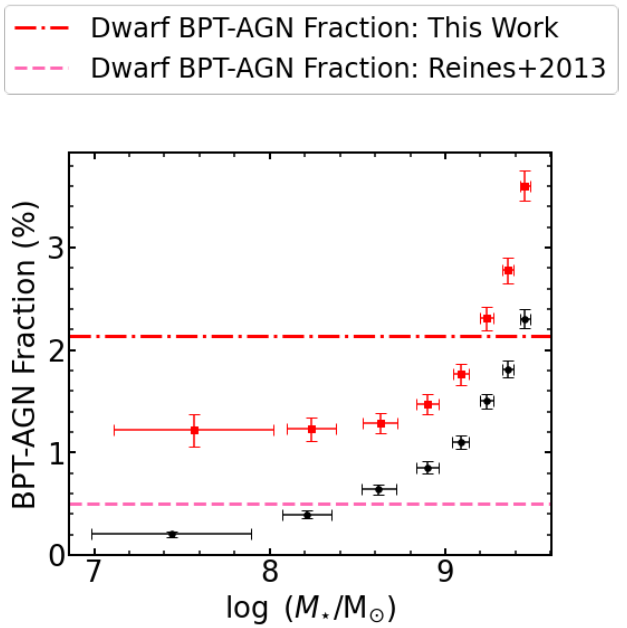

Масса ЧД – по сути, “метод Дибая”

$$M_{\rm BH} \propto \frac{RV^2}{G}$$

2022), we use the Greene & Ho (2005) formula for estimating the BH masses, with the modified radius-luminosity relationship of Bentz et al. (2013) as derived by Reines et al. (2013):

$$\log\left(\frac{M_{\rm BH}}{\rm M_\odot}\right) = \log\epsilon + 6.57 + 0.47\log\left(\frac{L_{\rm H\alpha;b}}{10^{42}\ \rm erg\ s^{-1}}\right) + 2.06\log\left(\frac{\rm FWHM_{H\alpha;b}}{10^{3}\ \rm km\ s^{-1}}\right)$$

FWHM of the broad Hα component and ϵ is the scale factor, which spans a range of ~0.75–1.4 (Greene & Ho

Метод Дибая (спектр одной эпохи)

$$M_{\rm BH} = f\frac{R_{\rm BLR}\cdot\sigma_v^2}{G}$$

Дибай (1977):
По сути, то же соотношение, но R оценивалось из объема излучающего ионизованного газа:

$L(H\beta)\sim\varepsilon n_e^2 R^3$
$n_e=3\cdot10^8$ см$^{-3}$, $\varepsilon=0.001$

В похожих вариациях массово применяется и сейчас

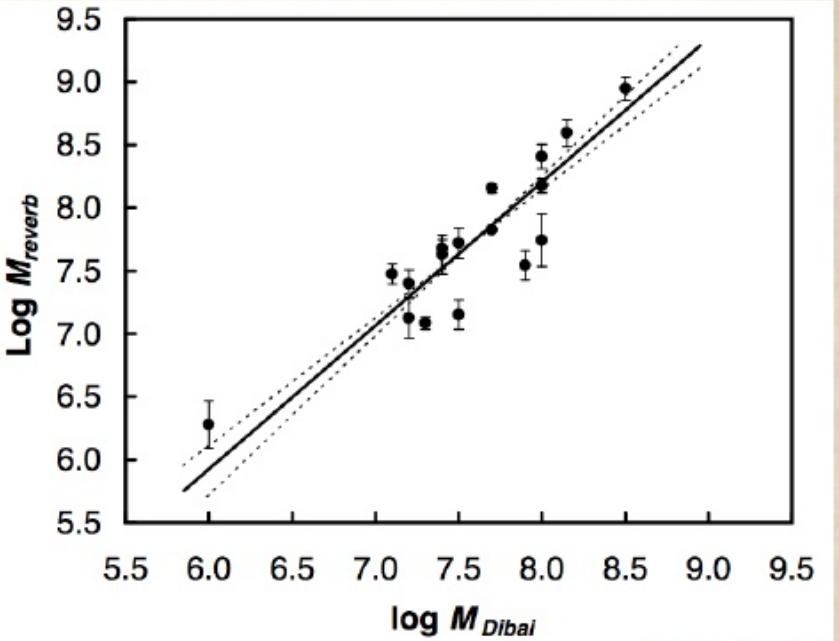

FIG. 1.— Comparison of the mass estimates of Dibai (1984b), M_{Dibai} with reverberation mapping masses, M_{reverb}. The solid

(Bochkarev & Gaskell 2009)

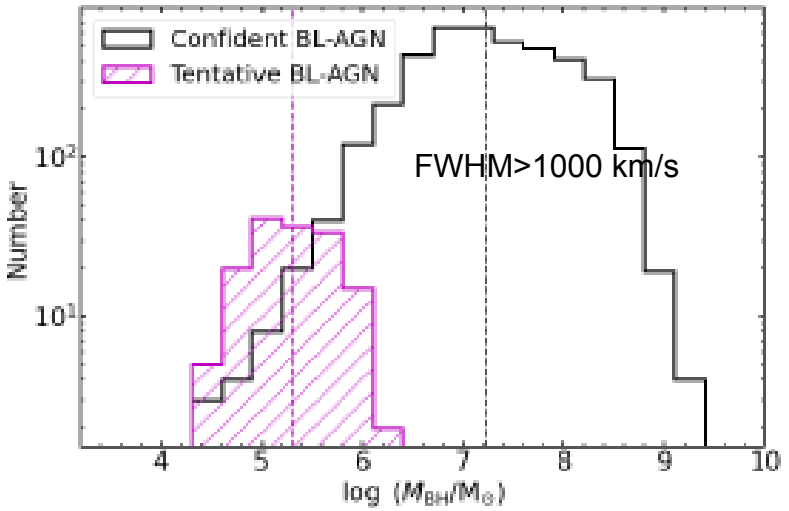

IMBH (lg M<6): 151 confident + 147 tentative candidates

QSO?
=> неуверенная оценка массы

Разделение типов по Сersику n=2

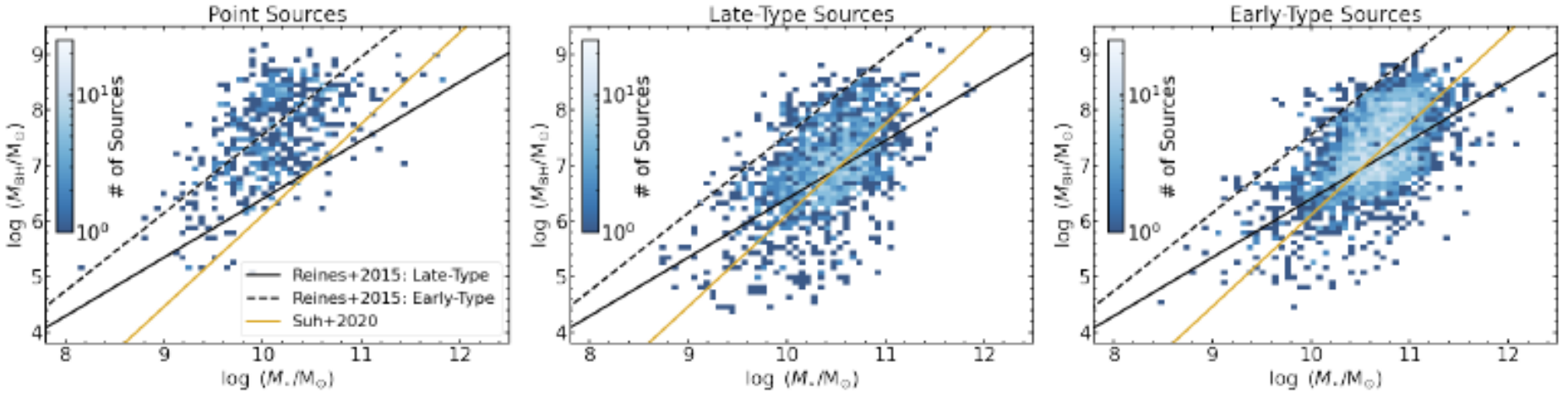

Без звездообразных источников

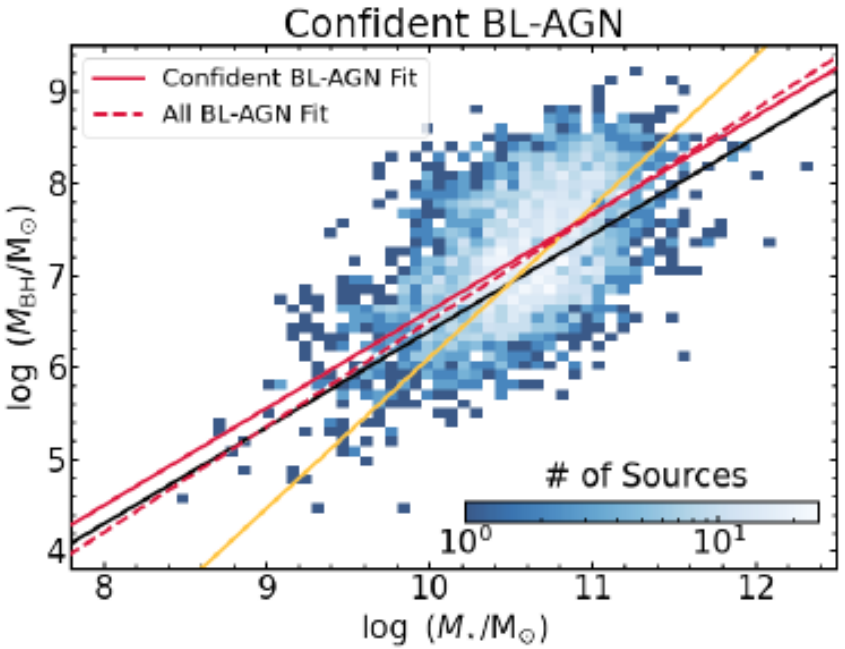

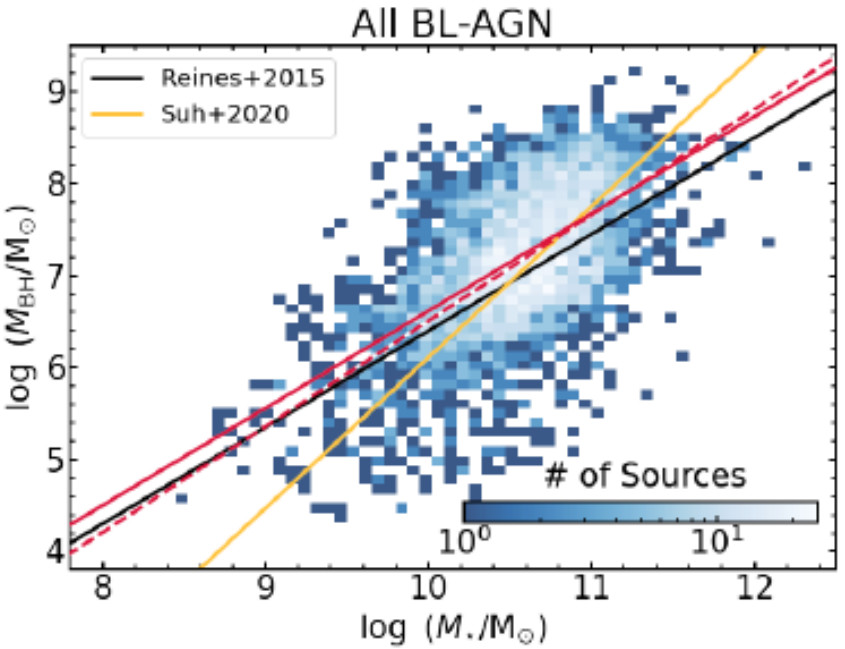

$$\log(M_{\rm BH}/{\rm M}_\odot) = \alpha + \beta \log(M_\star/10^{11}{\rm M}_\odot) \quad (2)$$

Considering only the confident BL-AGN candidates, we find:

$$\alpha = 7.67 \pm 0.01; \beta = 1.05 \pm 0.02 \quad (3)$$

When we consider all the BL-AGN candidates, we find:

$$\alpha = 7.66 \pm 0.01; \beta = 1.15 \pm 0.03 \quad (4)$$

Нет выхолаживания соотношения на малых массах – аргумент в пользу “heavy seeds” (прямой коллапс газа), против “light seeds” (Pop III)

Сравнение с SDSS (dwarf AGN: 0.5 vs 2.1%)

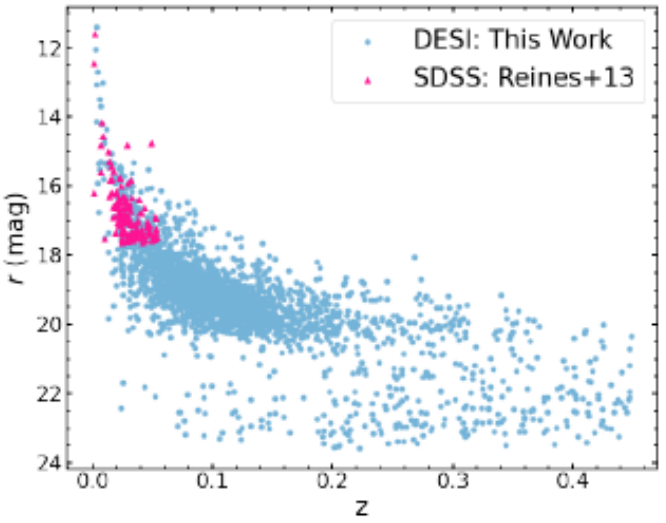

Figure 13. Distribution of dwarf AGN candidates from this work (shown as blue circles) and from Reines et al. (2013) (shown as pink triangles) in the $r - z$ space. Our sample of dwarf AGN candidates extend down to fainter magnitudes and to higher redshifts compared to the ones identified by Reines et al. (2013).

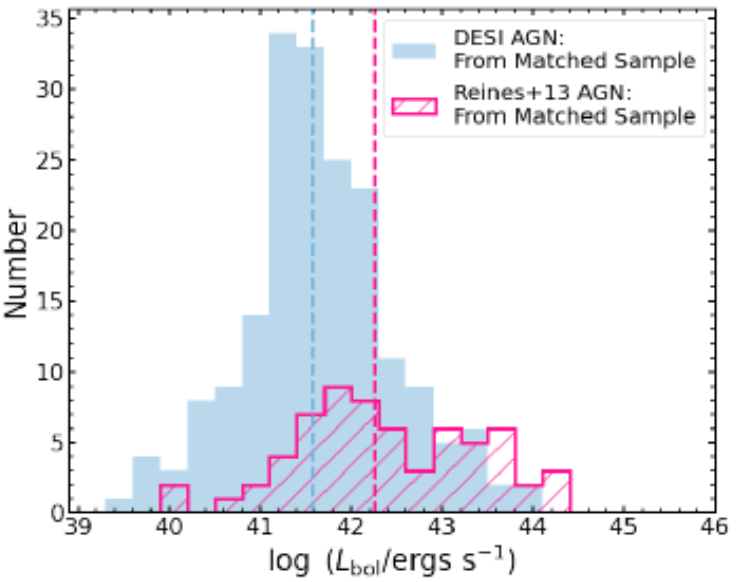

Figure 14. Distribution of AGN bolometric luminosities of the dwarf AGN candidates from the matched starting sample between DESI and SDSS. The filled blue histogram shows the dwarf AGN candidates from DESI, while the

Сильно продвинулись в сторону тусклых и далеких галактик, при этом:

- DESI выше разрешение: 60 – 150 км/с vs 100-190
- Тоньше волокно (1.5 vs 3") – меньше вклад от ЗО в галактике

Основные выводы

- Using the optical emission-line [NII]-BPT diagnostic, we find 75,928/296,261 (≈25.6%) high-mass AGN candidates and 2,444/114,496 (≈2.1%) dwarf AGN candidates. With these sources, we have more than tripled the existing census of optical dwarf AGN candidates (Section 4).

Но за AGN принимают и все композитные ядра
Чисто оптическая выборка

- Our estimation of the dwarf BPT-AGN fraction (≈2.1%) is nearly four times higher than that from a comparable systematic search using SDSS (Reines et al. 2013). This increase can be primarily attributed to the smaller fiber size of DESI compared to SDSS, which aids with the identifi-

Апертурный эффект в чистом виде. Интересно сравнить с выборками по IFU

- We find that the BPT-AGN fraction in line emitting galaxies increases with increasing stellar mass, from ≈1.2% at $\log(M_\star/\mathrm{M}_\odot)$ ≈8.0 to ≈93.5% at $\log(M_\star/\mathrm{M}_\odot)$ ≈11.4. On average, the BPT-AGN fraction slightly decreases with increasing redshift. However, these trends are affected by selection effects including stellar mass variations, emission line detection limits, and DESI targeting algo-

Для всех, а не только эмиссионных галактик – цифры скромнее. И мощные эффекты селекции

- We estimate the BH masses of the BL-AGN candidates using the flux and width measurements of the broad Hα component. The BH masses extend down to $\log(M_{\mathrm{BH}}/\mathrm{M}_\odot) \approx 4.4$ for confident BL-AGN candidates and to $\log(M_{\mathrm{BH}}/\mathrm{M}_\odot) \approx 4.3$ for tentative candidates. Among these, we find 151 confident (and 147 tentative) BL-AGNs have $M_{\mathrm{BH}} \leq 10^6\ \mathrm{M}_\odot$, making this the largest sample of IMBH candidates to date (Section 5.1).

Важно, что в тексте (в отличие от пресс-релизов) аккуратно подчеркивается, что все это пока лишь кандидаты. И зависимость от массы галаткики сильно размыта, сравнительно с σ-M(BH)

Во всем обзоре обещают (2026) обещают
>10 000 dwarf AGN candidates

- We extend the $M_{\mathrm{BH}} - M_\star$ scaling relation down to $\log(M_\star/\mathrm{M}_\odot) \approx 8.5$ and $\log(M_{\mathrm{BH}}/\mathrm{M}_\odot) \approx 4.4$ (Figure 11). The empirical fit from these sources has a similar slope to Reines & Volonteri (2015), but a slightly higher normalization (Section 5.3).